et al., 2005). Further, it was revealed that the oral administration of L-745,870 attenuated ischemia-induced damage of the hippocampus CA1 neurons in a gerbil model (Okada et al., 2005). Taken together, L-745,870 may have a potency in the treatment of neurodegenerative diseases associated with oxidative stress, such as ALS.

Therefore, the aim of the present study was to investigate the efficacy of L-745,870 in the treatment of ALS through the study in which the systemic administration of L-745,870 to mice expressing a mutated form of human *SOD1* gene ($SOD1^{H46R}$) was conducted. We here demonstrated that the pre-onset administration of L-745,870 significantly retarded the disease-onset and prolonged survival in transgenic $SOD1^{H46R}$ mice. The L-745,870 treatment also delayed loss of motor neurons in the spinal cord accompanying with the reduced level of microglial activation and TNF-α expression. Intriguingly, the post-onset administration of L-745,870 resulted in a slowed progression and prolongation of a post-onset survival span in a same mouse ALS model. Collectively, L-745,870 may provide a novel therapeutic means towards the treatment of ALS.

Materials and methods

Chemicals and antibodies

3-{[4-(4-chlorophenyl)piperazin-1-yl]methyl}-1*H*-pyrrolo[2,3-*b*] pyridine (L-745,870) (Molecular Weight: 326.82) was purchased from Ishihara Sangyo Kaisha, LTD (Siga, Japan), and subjected to animal experiments. All other chemicals are from commercial sources and of analytical grade. Antibodies used in this study included rabbit polyclonal anti-SOD1 antibody (#sc-11407; Santa Cruz), rabbit polyclonal anti-ionized calcium binding adaptor molecule 1 (Iba-1) antibody (#019-19741; Wako), rabbit polyclonal anti-glial fibrillary acidic protein (GFAP) antibody (#RB-087-A0; LAB VISION), anti-mouse TNF-α/TNFSF1A antibody (AF-410-NA; R&D SYSTEMS), and anti-nitrotyrosine antibody (#06-284, UPSTATE).

Animals

In this study, we used transgenic mice carrying the H46R mutation in the human *SOD1* gene; $SOD1^{H46R}$ (Chang-Hong et al., 2005; Sasaki et al., 2007) as a model for fALS. Since genetic background is one of the important factors modulating disease phenotypes in mutant *SOD1* transgenic mice (Heiman-Patterson et al., 2005), we first generated congenic line of $SOD1^{H46R}$ transgenic mice by backcrossing more than 12 generations with C57BL/6N mice, and then the line was maintained as hemizygotes by mating $SOD1^{H46R}$ males with C57BL/6N females. The offsprings were genotyped by a PCR assay using genomic DNA from tail tissue. Mice were housed at an ambient temperature of 23 °C and at a 12 h light/dark cycle, in which water and food were available *ad libitum*. All animal experimental procedures were approved by the Tokai University Medical School Committee on Animal Care and Use.

Administration of the compound

L-745,870 was dissolved in 0.233 N HCl and then adjusted at an appropriate concentration by diluting with physiological saline. Animals were anesthetized with halothane (4%) in a mixture of N_2O/O_2 (70:30), and were intragastrically (i.g.) received with L-745,870 via a gastric tube (CAT.No.4202, Fuchigami) at a dose of either 4 mg/kg, 10 mg/kg or 20 mg/kg body weight. In parallel, two different control groups of animals; those treated with anesthesia alone (sham group) and with anesthesia followed by the vehicle administration (vehicle group), were adopted. The daily administration of L-745,870 or vehicle to mice was conducted starting at 12 weeks of age (pre-onset administration) or at the day at which animals exhibited a sign of motor dysfunction (see bellow); the onset (post-onset administration), and was continued until their terminal phase (death).

Observation of gross phenotypes in mice

Body weight of each mouse was measured from 12 weeks of age and weekly thereafter until death. Gross behavior of each animal was daily observed through visual inspection. In particular, hind limb movement and rearing behavior of each animal were weekly monitored by video camera from 12 weeks of age to the end stage. To determine the age at onset of motor dysfunction in transgenic mice, we adopted a balance beam test using the stainless steel bar (45 cm long and 0.9 cm in diameter). Motor function in the hind limbs was assessed at 12 weeks of age, and weekly thereafter until the day at which mice were unable to stay on the bar. We used the following five arbitrary grades to evaluate the motor function of mice; grade 5 (enable to walk and change the directions on the bar without their hind limb slipping), grade 4 (occasionally showed a sign of hind limb slipping, but skillfully walk on the bar), grade 3 (frequently showed a hind limb slipping, but still awkwardly walked on the bar), grade 2 (stay on the bar, but quickly fall off from the bar when attempt to walk), and grade 1 (unable to stay on the bar). In this study, the grade 3 was defined as the sign of the disease onset. Lifespan of animals was determined by the observations that mice have no longer had a heartbeat and breathing, and survival interval was calculated by the subtraction of the day of life span by the day of disease onset.

Assessment of motor function

We assessed motor performance, coordination, and balance of mice using the rotarod apparatus (MK-660A, Muromachi Kikai Co. Ltd, Japan). The duration retaining on a rod (diameter, 30 mm; rotation speed, 8 rpm; a maximum period, 120 s) without falling was measured. After the training session (20 rpm × 5 trails for 2 days), mice were tested once a week until they could no longer perform the task. Each mouse was given five trials, and the longest duration on the rod was scored.

Western blot analysis

At 13 weeks (pre-symptomatic stage; 1 week after the initial administration of L-745,870) and 22 weeks (late-symptomatic stage; after the administration of L-745,870 over a period of 10 weeks) of ages, the mice were anesthetized with halothane (4%) in a mixture of N_2O/O_2 (70:30) and transcardially perfused with physiological saline containing 10% heparin, and lumbar spinal cord was removed. Tissues were homogenized in lysis buffer (50 mM Tris–HCl (pH 7.5), 150 mM NaCl, 0.1% NP-40, Complete Protease Inhibitor Cocktail (Roche)), and was centrifuged at 22,000 ×g for 30 min. The resultant supernatant was collected as a NP-40 soluble fraction. The insoluble pellet fraction was then suspended with phosphate-buffered saline (PBS) (pH 7.2) containing 5% sodium dodecyl sulfate (SDS), sonicated, and left for 30 min at room temperature. After the centrifugation at 22,000 ×g for 30 min, the supernatant was collected as a SDS-soluble fraction. Protein concentration of each fraction was determined by the Micro BCA system (Pierce). Ten μg of protein from each fraction was electrophoretically separated on a 15% SDS-polyacrylamide gel, and transferred onto polyvinylidene difluoride (PVDF) membrane (Bio-Rad Laboratories, Hercules, CA). Membrane was blocked with 5% skimmed-milk (Wako) in TBST buffer (50 mM Tris–HCl (pH 7.4), 150 mM NaCl, 0.1% (w/v) Tween-20) overnight at 4 °C and was then incubated with the anti-SOD1 antibody (dilution 1:10,000) in TBST containing 1% skimmed-milk for 2 h at room temperature. After washing with TBST, membranes were incubated with the peroxidase-conjugated secondary anti-rabbit IgG (#NA934, GE Healthcare UK Ltd, Buckinghamshire, UK) for 1 h at room temperature. Signals were detected using ECL Plus (GE Healthcare UK Ltd).

Histopathological analysis

At 13 weeks, 19 weeks, and 22 weeks of ages, the mice were anesthetized with halothane (4%) in a mixture of N_2O/O_2 (70:30).

Under the anesthesia, the mice were transcardially perfused with physiological saline containing 10% heparin, followed by 4% paraformaldehyde (PFA) in 0.1M phosphate buffer (PB) (pH 7.2). Spinal cord was removed and post-fixed with the same fixative for 48 h at 4 °C. Lumbar segment (3–4 mm in length) was embedded in paraffin. Serial transverse sections (6 μm thickness) of lumbar segment (L4) were sliced and stained with hematoxylin and eosin (H&E) for histopathological evaluation.

Quantitative assessment of the number of anterior horn neurons in L4 lumbar segment from mice at 22 weeks of age was also conducted. Sections (6 μm thickness) were stained with cresyl-violet (Nissl staining) and observed under light microscope equipped with a CCD camera (DP71, OLYMPUS). A total of 9 representative images of every sixth serial section throughout L4 segment was analyzed. A size of neuron (cross-sectional area of each soma) was also determined by utilizing ImageJ software version 1.33u (NIH). The anterior horn neurons were counted as those fulfilled the following three criteria; 1) neurons located within ventral half of the gray matter of the spinal cord (see Fig. 4D), 2) neurons with distinct nucleolus, and 3) neurons whose the cross-sectional area was over 40 μm^2.

Immunohistochemical analysis

Immnohistochemical analyses with anti-Iba-1 (dilution 1:200), anti-GFAP (dilution 1:200), anti-TNF-α (dilution 1:50), and anti-nitrotyrosine (dilution 1:50) antibodies were performed. For immunostaining using anti-Iba-1 antibody, but not using anti-GFAP antibody, the deparaffinized sections from 22 weeks of age were pre-treated by autoclaving at 121 °C for 5 min in 10 mM citrate buffer (pH 6.0). The sections were incubated with 0.3% H_2O_2 in methanol for 30 min and then with phosphate-buffered saline (PBS) (pH 7.2) containing 0.3% Triton X-100 for 30 min. After the treatment with PBS containing 5% normal goat serum (NGS) (S-1000, Vector Laboratories) for 1 h at room temperature, the sections were incubated with either anti-Iba-1 or anti-GFAP antibody in PBS containing 1.5% NGS and 0.05% Triton X-100 overnight at 4 °C. The sections were then incubated with HISTOFINE simple stain mouse MAX-PO (R) (code 414341, Nichirei Corporation, Japan) overnight at 4 °C. The sections were visualized using 0.05% 3,3-diaminobenzidine tetrahydrochloride (DAB) (Wako) and 0.015% H_2O_2 in 50 mM Tris–HCl (pH 7.5) buffer, and the DAB reaction products were observed under a microscope.

For immunostaining using anti-TNF-α and anti-nitrotyrosine antibodies, microwave treatment of the sections from 19 weeks of age was performed for 5 min in 10 mM citrate buffer (pH 6.0). The sections were then incubated with 3% H_2O_2 for 30 min and with PBS (pH 7.2) containing 0.3% Triton X-100 for 30 min. After the treatment with PBS containing 5% normal rabbit serum (NRS) (S-5000, Vector Laboratories) or 5% NGS for 1 h at room temperature, the sections were incubated with anti-TNF-α antibody in PBS containing 1.5% NRS and 0.05% Triton X-100 or with anti-nitrotyrosine antibody in PBS containing 1.5% NGS and 0.05% Triton X-100 overnight at 4 °C. The sections were then incubated with HISTOFINE simple stain mouse MAX-PO (G) (code 414351, Nichirei Corporation, Japan) or with HISTOFINE simple stain mouse MAX-PO (R) overnight at 4 °C, and were visualized using DAB. The DAB reaction products were observed under a microscope.

Statistical analysis

Data in this study were presented as mean±SD or mean±SEM. Statistical significance was evaluated by ANOVA (analysis of variance) followed by Tukey's method for multiple comparisons between groups (Microsoft Office Excel 2003 with Excel statistics 2006). Survival data were compared using Kaplan–Meier survival analysis with log-rank test (SPSS 15.0J software). A P-value <0.05 was

Results

The L-745,870 treatment improves clinical symptoms in SOD1^{H46R} mice

In SOD1^{H46R} mice (Chang-Hong et al., 2005; Sasaki et al., 2007), the first sign of disease symptom was weakness of hind limbs, which was observed at ~17 weeks of age. As the disease progresses, abnormal gait became more apparent, and hind limb movement and rearing activity were progressively impaired. Further, when suspended by the tail, SOD1^{H46R} mice exhibited the feet-clasping like posture at an early

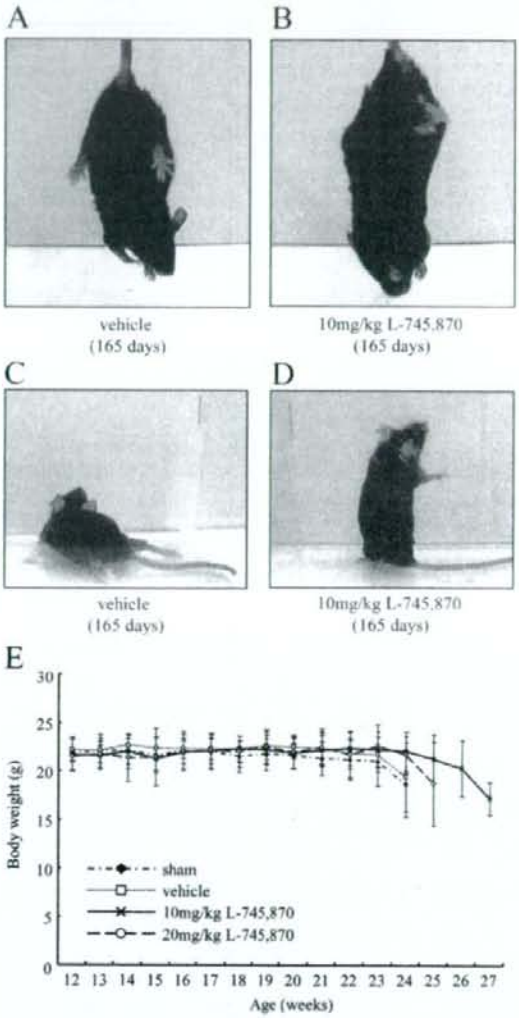

Fig. 1. Effect of the L-745,870 treatment on the gross clinical symptoms in SOD1^{H46R} mice. (A and B) Representative photographs of mice at 165 days of age showing a typical hind limb posture upon the tail suspension. The vehicle-treated mouse shows a complete paralysis in hind limb (A), whereas the L-745,870-treated mouse (10 mg/kg) still exhibits a feet-clasping phenotype (B). (C and D) Representative photographs of mice at 165 days of age showing a rearing behavior. The vehicle-treated mouse is unable to keep an upright posture (C), while those treated with L-745,870 shows a rearing behavior (D). (E) Changes in the body weight of SOD1^{H46R} mice in sham, vehicle, and L-745,870 (10 mg/kg or 20 mg/kg)-treated groups (each $n=8$). Data are expressed as mean±SD. No statistically significant differences between experimental groups were observed throughout experimental periods (12–27 weeks of age) (ANOVA). Nevertheless, it is notable that a reduction (approximately 10%) of body weight observed at the end stage of disease (23–24 weeks of

symptomatic stage, while non-transgenic litters showed a laterally extended posture of their hind limbs (data not shown). At the end stage of disease (~23 weeks of age), they showed a complete paralysis; no movement of hind limbs, upon the tail suspension. Ultimately, the mice were unable to move and died at ~24 weeks of age.

To evaluate the effect of L-745,870 on disease symptoms, the treatment of SOD1^{H46R} mice with L-745,870 was initiated at 12 weeks of age (pre-symptomatic stage). The mice were received with L-745,870 daily at a dose of either 10 mg/kg or 20 mg/kg body weight, and were monitored their hind limb movement and rearing activity. At 23 weeks of age, a majority of the vehicle-treated mice showed a complete paralysis of hind limbs, and thus never showed a feet-clasping phenotype upon the tail suspension and a rearing behavior (Fig. 1A and C). In contrast, the L-745,870-treated mice at the same age still showed a feet-clasping phenotype and rearing activity (Fig. 1B and D).

As SOD1^{H46R} mice had already reached their maximum body weight at 12 weeks of age, the effect of the L-745,870 on the weight gain could not be evaluated in this study. However, the treatment of L-745,870 prevented SOD1^{H46R} mice from early weight loss (Fig. 1E) by retarding the disease progression. Incidentally, non-transgenic littermates treated

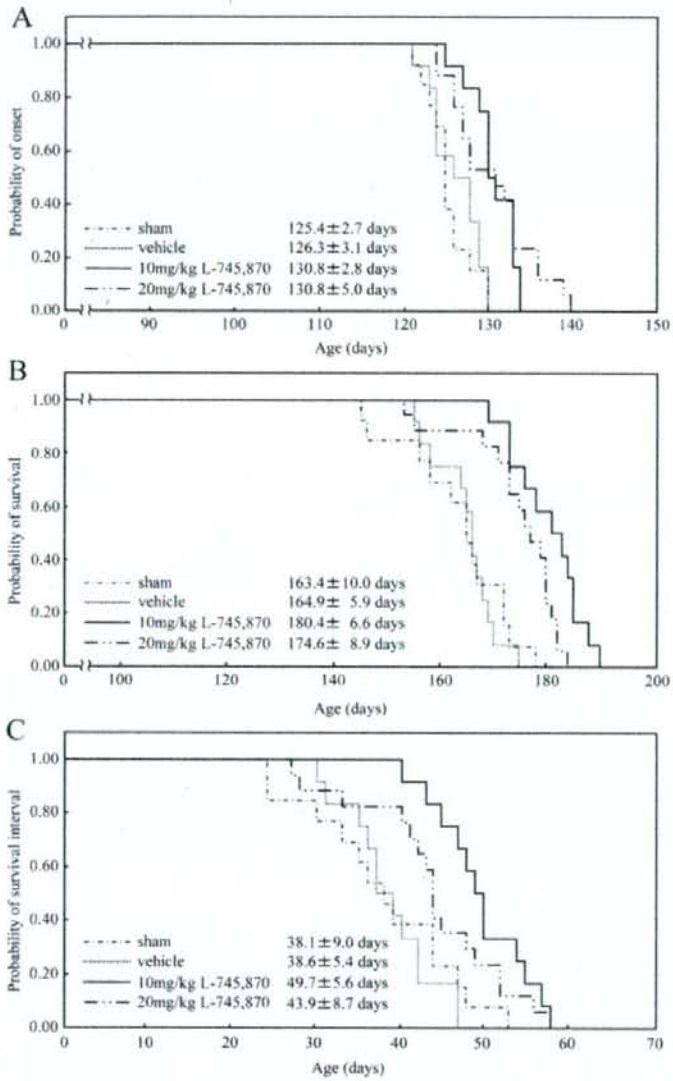

Fig. 2. Effect of the L-745,870 treatment on the disease onset and survival of SOD1^{H46R} mice. The Kaplan–Meier curves demonstrate the probability of onset (A), survival (B), and survival interval (C) for sham control (n = 13), vehicle control (n = 12), 10 mg/kg L-745,870-treated (n = 12), and 20 mg/kg L-745,870-treated (n = 17) SOD1^{H46R} mice. (A) The onsets were significantly delayed in 10 mg/kg and 20 mg/kg L-745,870-treated groups compared with sham control group (P < 0.001 and P = 0.001 by log-rank test, respectively), and in 10 mg/kg and 20 mg/kg L-745,870-treated groups compared with vehicle control group (P = 0.001 and P = 0.006 by log-rank test, respectively). (B) The life spans for both 10 mg/kg and 20 mg/kg L-745,870-treated groups were significant longer than those for sham and vehicle control groups (P < 0.001 by log-rank test). (C) Survival intervals after the onset were prolonged in 10 mg/kg L-745,870-treated group compared with either sham (P = 0.001 by log-rank test) or vehicle control group (P < 0.001 by log-rank test), and in 20 mg/kg L-745,870-treated group compared with vehicle control group (P = 0.013 by log-rank test). Value of the mean ± SD in each experimental group is also indicated.

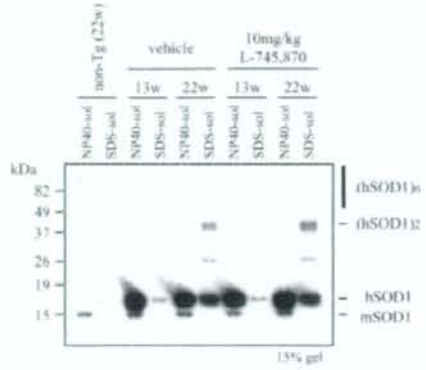

Fig. 3. Effect of the L-745,870 treatment on the mutant SOD1 level. The expression of the SOD1 protein in lumbar spinal cord from SOD1^{H46R} mice (13 or 22 weeks of age) treated with vehicle or L-745,870 (10 mg/kg) and from non-transgenic (non-Tg) littermates (22 weeks of age) were examined by Western blot analysis using anti-SOD1 antibody. Tissue extracts were separated into two fractions by centrifugation; NP-40 soluble fraction (NP40-sol) and NP-40-insoluble/SDS-soluble fraction (SDS-sol). hSOD1 and mSOD1 represent the mutated (H46R) human SOD protein and endogenous mouse SOD1 protein, respectively. $(hSOD1)_2$ and $(hSOD1)_n$ indicate the dimerized and oligomerized forms of SOD1, respectively.

with L-745,870 exhibited no observable abnormalities (data not shown), indicating that the doses of the compound used in this study are not harmful to mice. Taken together, the L-745,870 treatment might improve clinical symptoms in SOD1^{H46R} mice.

The administration of L-745,870 delays disease onset and progression

We next evaluated the effect of L-745,870 on the disease onset and progression in SOD1^{H46R} ALS mice using the Kaplan–Meier survival analysis. The disease onset was defined at which mice showed symptom of grade 3 in balance beam test (see Materials and Methods). The mean onsets of disease for both 10 mg/kg and 20 mg/kg L-745,870-treated groups (130.8±2.8 and 130.8±5.0 postnatal days, respectively) were significantly delayed when compared with those for either sham (125.4±2.7 days) or vehicle group (126.3±3.1 days) (Fig. 2A). The life spans for both 10 mg/kg and 20 mg/kg L-745,870-treated groups (180.4±6.6 days and 174.6±8.9 days, respectively) were significantly longer than those for sham and vehicle groups (163.4±10.0 days and 164.9±5.9 days, respectively) (Fig. 2B). Further, survival intervals after the onset in L-745,870-treated animals, particularly those treated at a dose of 10 mg/kg (10 mg/kg; 49.7±5.6 days and 20 mg/kg; 43.9±8.7 days) were extended when compared with those in sham and vehicle groups (38.1±9.0 days and 38.6±5.4 days, respectively) (Fig. 2C). These results indicate that L-745,870 acts as a protective reagent against not only the onset of motor dysfunction but also the disease progression in SOD1^{H46R} mice.

The L-745,870 treatment does not alter the SOD1 protein level

To ensure that the administration of L-745,870 had not altered the expression of the human *SOD1* transgene in SOD1^{H46R} mice, we examined the levels of the SOD1 protein in the lumbar spinal cord by Western blot analysis (Fig. 3). Endogenous mouse SOD1 (mSOD1) was

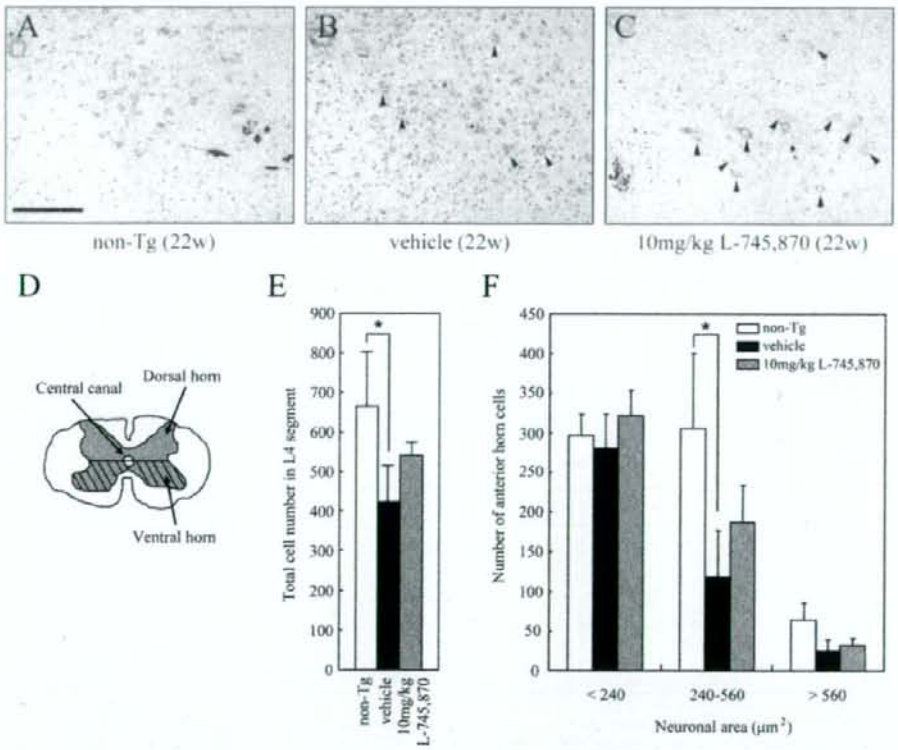

Fig. 4. Effect of the L-745,870 treatment on motor neuron loss in the spinal cord. (A–C) Representative images for the Nissl-staining of the anterior horn in the lumbar (L4) spinal cord prepared from non-transgenic (non-Tg) (A), vehicle-treated SOD1^{H46R} (B), and L-745,870-treated (10 mg/kg) SOD1^{H46R} (C) mice at 22 weeks of age. Arrowheads indicate spinal motor neurons. Scale bar indicates 200 μm. (D) Schematic representation of the cross-sectional L4 segment of the lumbar spinal cord. The number of the neurons within the hatched region was counted. (E) The total number and (F) the size distribution of anterior horn cells (≥40 μm²) within the ventral half of the gray matter (hatched region shown in D) in the L4 lumbar spinal cord of non-Tg (n=3), vehicle-

present in the NP-40 soluble fractions from all animals including non-transgenic litters, while mutated human SOD1 (hSOD1) was only detected in the samples from SOD1^{H46R} mice. There were no significant differences in the mutant SOD1 levels from the NP-40 soluble fractions between vehicle- and L-745,870-treated groups either at 13 weeks or 22 weeks of age. Further, although the levels of the NP-40-insoluble/SDS-soluble SOD1 protein were increased at 22 weeks of age when compared at 13 weeks of age, no significant differences in their levels between experimental groups were observed. These results indicate that L-745,870 has no apparent effect on the mutant SOD1 expression, and that the improvement of disease symptom in the L-745,870-treated animals observed in this study is not simply due to the decreased level of the mutant SOD1 protein.

The L-745,870 treatment protects from motor neuron loss

To determine whether the protective effect of L-745,870 from the progression of motor dysfunction was due to the delayed motor neuron loss, we evaluated the number of motor neurons in the spinal cord. Non-transgenic and SOD1^{H46R} mice had similar motor neuron numbers at 13 week of age (pre-onset stage; data not shown). In contrast, at a late symptomatic stage (22 weeks of age), SOD1^{H46R} mice treated with vehicle showed an extensive loss of large anterior horn cells (Fig. 4B) compared with non-transgenic littermate (Fig. 4A). Notably, large anterior horn cells of SOD1^{H46R} mice treated with L-745,870 were relatively spared (Fig. 4C), suggesting that L-745,870 protected motor neurons from loss at a late symptomatic stage.

To confirm this notion, we conducted a quantitative analysis of the number of motor neurons whose soma sizes were larger than 40 μm^2 in the anterior horn located within ventral half of the gray matter of the spinal cord (Fig. 4D). At 22 weeks of age, SOD1^{H46R} mice ($n=3$) with vehicle treatment showed a 36% loss of anterior horn cells when compared with non-transgenic littermates ($n=3$) (Fig. 4E). In contrast, L-745,870-treated SOD1^{H46R} mice ($n=3$) showed a 18% loss of anterior horn cells (Fig. 4E), and a significant difference was detected in the numbers of cells between non-transgenic and vehicle-treated groups ($p<0.05$; Fig. 4E). Further, while the numbers of large anterior horn cells (240–560 μm^2) in SOD1^{H46R} mice (vehicle controls) were

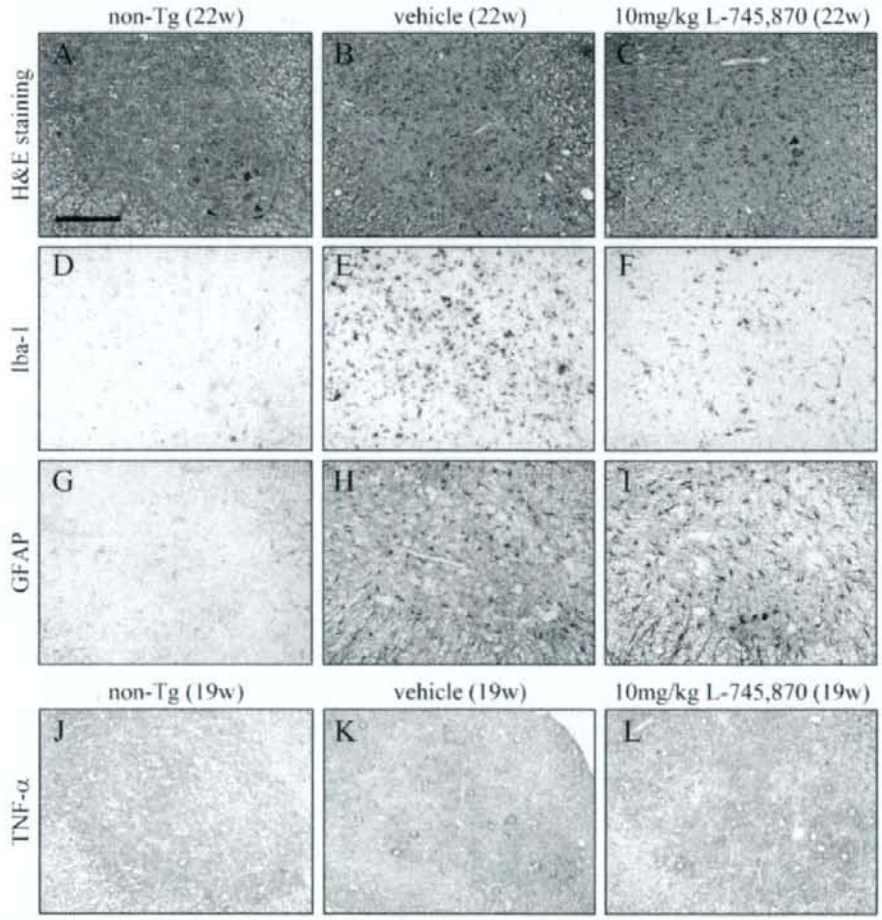

Fig. 5. Effect of the L-745,870 treatment on the activation of microglia and astrocyte and the expression of pro-inflammatory factor in the spinal cord. The lumbar spinal cord sections prepared from non-transgenic (non-Tg) (A, D, and G), vehicle-treated SOD1^{H46R} (B, E, and H), and L-745,870-treated (10 mg/kg) SOD1^{H46R} (C, F, and I) mice at 22 weeks of ages were stained with hematoxylin-eosin (H&E) (A–C), and immunostained with anti-Iba-1 (D–F) and anti-GFAP antibodies (G–I). The lumbar spinal cord sections prepared from non-Tg (J), vehicle-treated SOD1^{H46R} (K), and L-745,870-treated (10 mg/kg) SOD1^{H46R} (L) mice at 19 weeks of ages were immunostained with anti-TNF-α antibody (J–L). Scale bar indicates 200 μm.

preferentially decreased when compared with those in non-transgenic littermates (Fig. 4F), the L-745,870 treatment partly preserved such larger cells in SOD1^{H46R} mice (Fig. 4F). These results indicate that L-745,870 protects motor neurons in the spinal cord from progressive degeneration in an ALS mouse model.

The L-745,870 treatment suppresses microglial activation

Microglial activation occurs from early symptomatic stage in mutant SOD1 mice (Alexianu et al., 2001; Kriz et al., 2002). To assess whether the L-745,870 treatment affects the glial cell activation at sites of motor

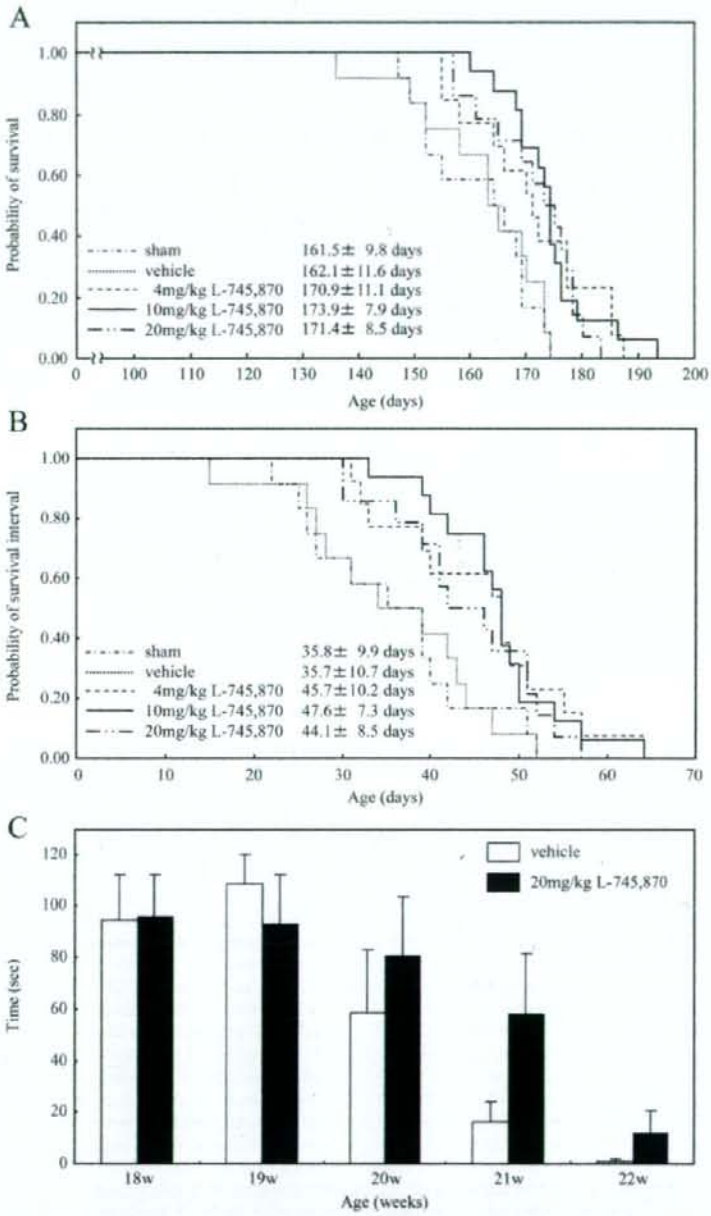

Fig. 6. Effect of the post-onset administration of L-745,870 on survival of SOD1^{H46R} mice. The Kaplan–Meier curves demonstrate the probability of survival (A) and survival interval (B) of sham control (n=12), vehicle control (n=12), 4 mg/kg L-745,870-treated (n=13), 10 mg/kg L-745,870-treated (n=16), and 20 mg/kg L-745,870-treated (n=14) SOD1^{H46R} mice. The average onset of SOD1^{H46R} mice was 125.9±2.8 days. (A) The life spans in L-745,870-treated groups at doses of 4 mg/kg, 10 mg/kg, and 20 mg/kg were significantly extended compared with sham group (P=0.018, P=0.001 and P=0.003 by log-rank test, respectively), and with vehicle group (P=0.042, P=0.002 and P=0.007 by log-rank test, respectively). (B) Survival intervals in L-745,870-treated groups at doses of 4 mg/kg, 10 mg/kg, and 20 mg/kg were significantly longer than those in sham group (P=0.038, P=0.012 and P=0.046 by log-rank test, respectively), and those in L-745,870-treated groups at doses of 4 mg/kg and 10 mg/kg were also longer than those in vehicle group (P=0.019 and P=0.003 by log-rank test, respectively). Value of the mean±SD in each experimental group is also indicated. (C) Effect of the L-745,870 treatment on the rotarod task in SOD1^{H46R} mice. The latencies to fall

neuron loss in SOD1^{H46R} ALS mice, we immunostained the lumbar sections of the spinal cord with anti-Iba-1 (marker for activated microglia) and anti-GFAP (marker for astrocytes) antibodies. At an early pre-symptomatic stage (13 weeks), there were no apparent differences in the immunoreactivity for either Iba-1 or GFAP in the lumbar spinal cord between non-transgenic, vehicle-treated SOD1^{H46R}, and L-745,870-treated SOD1^{H46R} mice (data not shown). In contrast, at 22 weeks of age (late symptomatic stage), vehicle-treated SOD1^{H46R} mice showed marked immunoreactivities both for Iba-1 and GFAP throughout the white and gray matters of the spinal cord with predominant localization in the anterior horn (Fig. 5E and H), where motor neurons were degenerated (Fig. 5B), while the lumbar spinal cord of non-transgenic siblings was almost devoid of those immunoreactivities (Fig. 5D and G). The results suggest a broad glial activation in the spinal cord of SOD1^{H46R} mice at this stage. Remarkably, L-745,870-treated SOD1^{H46R} mice showed a much less Iba-1 immunoreactivity in both white and gray matter of the anterior horn (Fig. 5F) and conservation of motor neurons (Fig. 5C) compared with vehicle-treated SOD1^{H46R} mice (Fig. 5B and E). However, there were no observable differences in immunoreactivities for GFAP, representing a diffused astrocytic proliferation in both groups (Fig. 5H and I). Immunoblot analysis also showed the decreased levels of Iba-1 in L-745,870-treated SOD1^{H46R} mice (data not shown). These results indicate that the L-745,870 treatment preferentially suppresses microglial activation, but not astrocytosis, in the spinal cord of SOD1^{H46R} mice.

The L-745,870 treatment suppresses the expression of pro-inflammatory factor

To confirm whether the L-745,870 treatment suppresses the expression of pro-inflammatory factor, we carried out immunostaining of the lumbar sections from spinal cord of SOD1^{H46R} ALS mice using anti-TNF-α antibody (Fig. 5J, K, and L). At 19 weeks of age, vehicle-treated SOD1^{H46R} mice showed marked immunoreactivities for TNF-α (Fig. 5K) particularly in large anterior horn cells, which was consistent with the recent findings (Bigini et al., 2008; Petri et al., 2007), compared with those in non-transgenic littermates (Fig. 5J). Notably, the TNF-α immunoreactivity in the corresponding region of L-745,870-treated SOD1^{H46R} mice was reduced (Fig. 5L). These results indicate that the L-745,870 treatment preferentially suppresses the expression of pro-inflammatory factor, such as TNF-α, in the spinal cord of SOD1^{H46R} mice.

We further assessed whether the L-745,870 treatment suppresses the protein oxidation in the spinal cord of SOD1^{H46R} ALS mice. Although the lumbar sections were broadly immunostained with anti-nitrotyrosine antibody, there were no significant differences of their immunoreactivities between vehicle-treated and L-745,870-treated SOD1^{H46R} mice (data not shown).

The post-onset administration of L-745,870 prolongs survival of SOD1^{H46R} mice

It is extremely crucial to evaluate whether the post-onset administration of L-745,870 improves disease symptoms. To address this issue, we conducted a daily administration of L-745,870 to SOD1^{H46R} mice after showing signs of onset (125.9±2.8 days) and observed disease progression and survival. The mean life spans (± SD) of the mice treated with 4 mg/kg, 10 mg/kg and 20 mg/kg of L-745,870 were 170.9±11.1, 173.9±7.9, and 171.4±8.5 days, respectively, and significantly extended when compared with sham (161.5±9.8 days) or vehicle-treated group (162.1±11.6 days) (Fig. 6A). Further, survival intervals in L-745,870-treated animals at doses of 4 mg/kg, 10 mg/kg, and 20 mg/kg (45.7±10.2, 47.6±7.3 and 44.1±8.5 days, respectively) significantly extended longer than those in sham (35.8±9.9 days) or vehicle-treated (35.7±10.7 days) mice (Fig. 6B), and were consistent with the results of the pre-onset administration of L-745,870 (Fig. 2C). The results also showed that 10 mg/kg of L-745,870 was an optimal dosage for exerting a potent neuroprotective efficacy in these experimental conditions. Thus, the post-onset administration of L-745,870 might effectively improve the disease symptoms and delays the disease progression in SOD1^{H46R} mice.

To further assess the effect of L-745,870 on symptoms, a rotarod test was conducted using the mice treated with L-745,870 after the onset. Although no statistically significant differences between vehicle control ($n=4$) and L-745,870-treated mice ($n=4$) were observed, there was a tendency showing that the motor function of L-745,870-treated mice was preserved when compared with that of vehicle control (Fig. 6C).

Discussion

ALS is a fatal neurodegenerative disease, and there are almost no effective therapeutic strategies to cure and/or relieve symptoms and improve the quality of life for patients to date. Although the mechanisms for the selective degeneration of motor neurons are still unclear, a complex interplay between multiple pathological factors, including oxidative stress, excitotoxicity, mitochondrial dysfunction, neurofilament accumulation, neural inflammation, and protein misfolding (Barber et al., 2006; Cluskey and Ramsden, 2001; Leichsenring et al., 2006; Menzies et al., 2002; Pasinelli and Brown, 2006; Shaw, 2005), is thought to associate with pathogenesis for ALS, and thus these factors are currently proposed as therapeutic targets. Among these pathogenic factors, there is substantial evidence to support the hypothesis that oxidative stress is one of the major processes implicating in the progression of motor neuron loss (Barber et al., 2006). This study aimed to explore the novel therapeutic agent which could alleviate oxidative stress-induced neural cell damage in ALS.

The small compound L-745,870, which is a dopamine D4 receptor antagonist having an excellent oral bioavailability and brain penetration, was firstly identified as a drug candidate for antipsychotic treatment (Patel et al., 1997). However, phase IIa clinical trials of L-745,870 failed to show clinical efficacy in patients with acute schizophrenia (Bristow et al., 1997). On the other hand, we previously reported that L-745,870 selectively inhibited cell death induced by oxidative stress *in vitro* and exerted a potent neuroprotective effect *in vivo* acute ischemic model (Okada et al., 2005). In the present study, we sought to examine whether the chronic administration of L-745,870 effectively attenuates motor neuron loss in a SOD1^{H46R} ALS mouse model. We here demonstrated that the pre-onset administration of L-745,870 significantly retarded the disease-onset and prolonged survival in transgenic SOD1^{H46R} mice. The L-745,870 treatment also delayed loss of motor neurons in the spinal cord accompanying with the reduced level of microglial activation. Most importantly, the post-onset administration of L-745,870 resulted in a slowed progression in a same mouse ALS model.

Currently, the pharmaco-mechanisms by which L-745,870 protects motor neuron loss are still unclear. In order to investigate the mode of action of L-745,870 *in vitro*, we previously performed cell viability analyses against cell death induced by various stimuli including oxidative stressors by utilizing non-neuronal (HeLa, THP-1, and fibroblast) and neuronal (SH-SY5Y) cell cultures. As a result, the L-745,870-treatment comparatively protected all examined cell types from death induced by oxidative stressors such as menadione and H_2O_2, but not by other stimuli such as staurosporine and okadaic acid (Okada et al., 2005), suggesting that L-745,870 selectively inhibited oxidative stress-induced cell death in a cell type-independent fashion. It has been reported that the several types of dopamine receptors are expressed in SH-SY5Y cells, but not in HeLa cells (Kamakura et al., 1997; Presgraves et al., 2004). Thus, L-745,870 seems to be effective to the cells irrespective to the expression of dopamine receptors. In other words, the mode of action of this compound could be dopamine receptor-independent, although we could not completely rule out the possibility that L-745,870 exerts its potency via dopamine receptors. Alternatively, as we have originally identified L-745,870 as a NAIP-upregulating compound (Okada et al., 2005), and NAIP is known to

exert potent neuroprotective activity against oxidative stress-induced cell death (Liston et al., 1996), it is reasonable that L-745,870 exerts its potency by enhancing the NAIP-mediated cellular protection from oxidative stress in transgenic SOD1^{H46R} mice.

Several lines of evidence have demonstrated that both microglia and astrocyte were proliferated in the affected regions of ALS patients and mutant SOD1 mouse ALS models (Hall et al., 1998; Kawamata et al., 1992; Schiffer et al., 1996). Two independent groups have reported that astrocytes have an impact on motor neuron degeneration (Di Giorgio et al., 2007; Nagai et al., 2007), while others have reported that microglia contribute to non-cell-autonomous damage of neurons in neurodegenerative diseases (Block et al., 2007; Liu and Hong, 2003; Moisse and Strong, 2006). Further, it has also been proposed that chromogranin-mediated secretion of mutant SOD1 from neurons and astrocytes enhances microgliosis and motor neuron death (Urushitani et al., 2006). These studies suggest a contribution of non-neuronal cells to the ALS pathogenesis. In the present study, we showed that L-745,870 suppressed the activation of microglia, but not astrocytosis, in the spinal cord of SOD1^{H46R} mice. Further, L-745,870 suppresses the upregulation of pro-inflammatory factor (TNF-α) but not the oxidative modification of proteins (nitrated proteins) in motor neurons. Recently, it has been reported that the activation of NADPH oxidase generating ROS from microglia promotes motor neuron degeneration in the spinal cord (Wu et al., 2006). NADPH oxidase, which is a membrane-bound enzyme and catalyzes the production of superoxide from oxygen, has been implicated as an important source of microglial-derived ROS generation (Block et al., 2007). It has also been shown that the production of pro-inflammatory factors is induced by ROS (Barber et al., 2006). Thus, the L-745,870 treatment may attenuate the microglia activation and coordinately suppress the expression of TNF-α in the spinal cord, which in turn results in the protection from motor neuron loss.

In conclusions, our findings in a rodent model of ALS, demonstrating an obvious neuroprotective efficacy of L-745,870, may have implication that L-745,870 is a promising candidate as a potential therapeutic drug to the treatment of ALS. Moreover, as reactive microglia have identified in the spinal cord from sporadic ALS patients (Kawamata et al., 1992), L-745,870 might be useful not only for familial but also for sporadic ALS. Although the mode of action of L-745,870 on motor neuron protection is not fully understood, future studies on the target analysis of L-745,870 *in vivo* will clarify more therapeutic potential of L-745,870 in ALS and other neurodegenerative diseases.

Acknowledgments

This work was funded by the Ministry of Health, Labour and Welfare (J.E.I.), and partly by the National Institute of Biomedical Innovation (NIBIO) (J.E.I.).

References

Alexianu, M.E., Kozovska, M., Appel, S.H., 2001. Immune reactivity in a mouse model of familial ALS correlates with disease progression. Neurology 57, 1282–1289.
Barber, S.C., Mead, R.J., Shaw, P.J., 2006. Oxidative stress in ALS: a mechanism of neurodegeneration and a therapeutic target. Biochim. Biophys. Acta 1726, 1051–1067.
Bigini, P., Repici, M., Cantarella, G., Fumagalli, E., Barbera, S., Cagnotto, A., De Luigi, A., Tonelli, R., Bernardini, R., Borsello, T., Mennini, T., 2008. Recombinant human TNF-binding protein-1 (rhTBP-1) treatment delays both symptoms progression and motor neuron loss in the wobbler mouse. Neurobiol. Dis. doi:10.1016/j.nbd.2007.11.005.
Block, M.L., Zecca, L., Hong, J.-S., 2007. Microglia-mediated neurotoxicity: uncovering the molecular mechanisms. Nat. Rev. Neurosci. 8, 57–69.
Bristow, L.J., Kramer, M.S., Kulagowski, J., Patel, S., Ragan, C.I., Seabrook, G.R., 1997. Schizophrenia and L-745,870, a novel dopamine D4 receptor antagonist. Trends Pharmacol. Sci. 18, 186–188.
Chang-Hong, R., Wada, M., Koyama, S., Kimura, H., Arawaka, S., Kawanami, T., Kurita, K., Kadoya, T., Aoki, M., Itoyama, Y., Kato, T., 2005. Neuroprotective effect of oxidized galectin-1 in a transgenic mouse model of amyotrophic lateral sclerosis. Exp. Neurol. 194, 203–211.
Cleveland, D.W., Rothstein, J.D., 2001. From Charcot to Lou Gehrig: deciphering selective motor neuron death in ALS. Nat. Rev. Neurosci. 2, 806–819.
Cluskey, S., Ramsden, D.B., 2001. Mechanisms of neurodegeneration in amyotrophic lateral sclerosis. J. Clin. Pathol: Mol. Pathol. 54, 386–392.
Di Giorgio, F.P., Carrasco, M.A., Siao, M.C., Maniatis, T., Eggan, K., 2007. Non-cell autonomous effect of glia on motor neurons in an embryonic stem cell-based ALS model. Nat. Neurosci. 10, 608–614.
Hall, E.D., Oostveen, J.A., Gurney, M.E., 1998. Relationship of microglial and astrocytic activation to disease onset and progression in a transgenic model of familial ALS. Glia 23, 249–256.
Heiman-Patterson, T.D., Deitch, J.S., Blankenhorn, E.P., Erwin, K.L., Perreault, M.J., Alexander, B.K., Byers, N., Toman, L., Alexander, G.M., 2005. Background and gender effects on survival in the TgN(SOD1-G93A)1Gur mouse model of ALS. J. Neurol. Sci. 236, 1–7.
Kamakura, S., Iwaki, A., Matsumoto, M., Fukumaki, Y., 1997. Cloning and characterization of the 5′-flanking region of human dopamine D4 receptor gene. Biochem. Biophys. Res. Commun. 235, 321–326.
Kawamata, T., Akiyama, H., Yamada, T., McGeer, P.L., 1992. Immunologic reactions in amyotrophic lateral sclerosis brain and spinal cord tissue. Am. J. Pathol. 140, 691–707.
Kim, N.H., Jeong, M.S., Choi, S.Y., Kang, J.H., 2004. Oxidative modification of neurofilament-L by the Cu,Zn-superoxide dismutase and hydrogen peroxide system. Biochimie 86, 553–559.
Kriz, J., Nguyen, M.D., Julien, J.-P., 2002. Minocycline slows disease progression in a mouse model of amyotrophic lateral sclerosis. Neurobiol. Dis. 10, 268–278.
Leichsenring, A., Linnartz, B., Zhu, X.R., Lübbert, H., Stichel, C.C., 2006. Ascending neuropathology in the CNS of a mutant SOD1 mouse model of amyotrophic lateral sclerosis. Brain Res. 1096, 180–195.
Liston, P., Roy, N., Tamai, K., Lefebvre, C., Baird, S., Cherton-Horvat, G., Farahani, R., McLean, M., Ikeda, J.-E., MacKenzie, A., Korneluk, R.G., 1996. Suppression of apoptosis in mammalian cells by NAIP and a related family of IAP genes. Nature 379, 349–353.
Liu, B., Hong, J.-S., 2003. Role of microglia in inflammation-mediated neurodegenerative diseases: mechanisms and strategies for therapeutic intervention. J. Pharmacol. Exp. Ther. 304, 1–7.
Menzies, F.M., Ince, P.G., Shaw, P.J., 2002. Mitochondrial involvement in amyotrophic lateral sclerosis. Neurochem.Int. 40, 543–551.
Moisse, K., Strong, M.J., 2006. Innate immunity in amyotrophic lateral sclerosis. Biochim. Biophys. Acta 1726, 1083–1093.
Nagai, M., Re, D.B., Nagata, T., Chalazonitis, A., Jessell, T.M., Wichterle, H., Przedborski, S., 2007. Astrocytes expressing ALS-linked mutated SOD1 release factors selectively toxic to motor neurons. Nat. Neurosci. 10, 615–622.
Okada, Y., Sakai, H., Kohiki, E., Suga, E., Yanagisawa, Y., Tanaka, K., Hadano, S., Osuga, H., Ikeda, J.-E., 2005. A dopamine D4 receptor antagonist attenuates ischemia-induced neuronal cell damage via upregulation of neuronal apoptosis inhibitory protein. J. Cereb. Blood Flow Metab. 25, 794–806.
Pasinelli, P., Brown, R.H., 2006. Molecular biology of amyotrophic lateral sclerosis: insights from genetics. Nat. Rev. Neurosci. 7, 710–723.
Patel, S., Freedman, S., Chapman, K.L., Emms, F., Fletcher, A.E., Knowles, M., Marwood, R., Mcallister, G., Myers, J., Curtis, N., Kulagowski, J.J., Leeson, P.D., Ridgill, M., Graham, M., Matheson, S., Rathbone, D., Watt, A.P., Bristow, L.J., Rupniak, N.M., Baskin, E., Lynch, J.J., Ragan, C.I., 1997. Biological profile of L-745,870, a selective antagonist with high affinity for the dopamine D4 receptor. J. PharmacolExp. Ther. 283, 636–647.
Petri, S., Calingasan, N.Y., Alsaied, O.A., Wille, E., Kiaei, M., Friedman, J.E., Baranova, O., Chavez, J.C., Beal, M.F., 2007. The lipophilic metal chelators DP-109 and DP-460 are neuroprotective in a transgenic mouse model of amyotrophic lateral sclerosis. J. Neurochem. 102, 991–1000.
Presgraves, S.P., Borwege, S., Millan, M.J., Joyce, J.N., 2004. Involvement of dopamine D(2)/D(3) receptors and BDNF in the neuroprotective effects of S32504 and pramipexole against 1-methyl-4-phenylpyridinium in terminally differentiated SH-SY5Y cells. Exp. Neurol. 190, 157–170.
Rao, S.D., Yin, H.Z., Weiss, J.H., 2003. Disruption of glial glutamate transport by reactive oxygen species produced in motor neurons. J. Neurosci. 23, 2627–2633.
Rao, S.D., Weiss, J.H., 2004. Excitotoxic and oxidative cross-talk between motor neurons and glia in ALS pathogenesis. Trends Neurosci. 27, 17–23.
Rosen, D.R., Siddique, T., Patterson, D., Figlewicz, D.A., Sapp, P., Hentati, A., Donaldson, D., Goto, J., O'Regan, J.P., Deng, H.-X., Rahmani, Z., Krizus, A., McKenna-Yasek, D., Cayabyab, A., Gaston, S.M., Berger, R., Tanzi, R.E., Halperin, J.J., Herzfeldt, B., Van den Bergh, R., Hung, W.-Y., Bird, T., Deng, G., Mulder, D.W., Smyth, C., Laing, N.G., Soriano, E., Pericak-Vance, M.A., Haines, J., Rouleau, G.A., Gusella, J.S., Horvitz, H., Brown Jr., R. R.H., 1993. Mutations in Cu/Zn superoxide dismutase gene are associated with familial amyotrophic lateral sclerosis. Nature 362, 59–62.
Sasaki, S., Nagai, M., Aoki, M., Komori, T., Itoyama, Y., Iwata, M., 2007. Motor neuron disease in transgenic mice with an H46R mutant *SOD1* gene. J. Neuropathol. Exp. Neurol. 66, 517–524.
Schiffer, D., Cordera, S., Cavalla, P., Migheli, A., 1996. Reactive astrogliosis of the spinal cord in amyotrophic lateral sclerosis. J. Neurol. Sci. 139 (Suppl.), 27–33.
Shaw, P.J., 2005. Molecular and cellular pathways of neurodegeneration in motor neurone disease. J. Neurol. Neurosurg. Psychiatry 76, 1046–1057.
Trotti, D., Rolfs, A., Danbolt, N.C., Brown Jr., R.H., Hediger, M.A., 1999. SOD1 mutants linked to amyotrophic lateral sclerosis selectively inactivate a glial glutamate transporter. Nat. Neurosci. 2, 427–433.
Urushitani, M., Sik, A., Sakurai, T., Nukina, N., Takahashi, R., Julien, J.-P., 2006. Chromogranin-mediated secretion of mutant superoxide dismutase proteins linked to amyotrophic lateral sclerosis. Nat. Neurosci. 9, 108–118.
Wu, D.-C., Ré, D.B., Nagai, M., Ischiropoulos, H., Przedborski, S., 2006. The inflammatory NADPH oxidase enzyme modulates motor neuron degeneration in amyotrophic lateral sclerosis mice. Proc. Natl. Acad. Sci. U.S.A. 103, 12132–12137.

Tohoku J. Exp. Med., 2008, **214**, 303-310

Up-Regulation of Insulin-Like Growth Factor-II Receptor in Reactive Astrocytes in the Spinal Cord of Amyotrophic Lateral Sclerosis Transgenic Rats

Byambasuren Dagvajantsan,[1] Masashi Aoki,[1] Hitoshi Warita,[1] Naoki Suzuki[1] and Yasuto Itoyama[1]

[1]Department of Neurology, Tohoku University Graduate School of Medicine, Sendai, Japan

Amyotrophic lateral sclerosis (ALS) is a fatal neurodegenerative disease caused by selective motor neuron death. We developed a rat model of ALS expressing a human cytosolic copper-zinc superoxide dismutase (SOD1) transgene with two ALS-associated mutations: glycine to alanine at position 93 (G93A) and histidine to arginine at position 46 (H46R). Although the mechanism of ALS is still unclear, there are many hypotheses concerning its cause, including loss of neurotrophic support to motor neurons. Recent evidence suggests that insulin-like growth factors (IGFs) act as neurotrophic factors, and promote the survival and differentiation of neuronal cells including motor neurons. Their ability to enhance the outgrowth of spinal motor neurons suggests their potential as a therapeutic agent for the patients with ALS. In this study, we investigated IGF-II receptor immunoreactivity in the anterior horns of the lumbar level of the spinal cord in SOD1 transgenic rats with the H46R mutation of different ages as well as in normal littermates. The double-immunostaining for IGF-II receptor and glial fibrillary acidic protein (GFAP) demonstrated co-localization on reactive astrocytes ($^{**}p < 0.001$) in the end-stage transgenic rats, whereas it was not evident at the pre-symptomatic stage or at the onset of the disease. Our results demonstrated the IGF-II receptor up-regulation in reactive astrocytes in the spinal cord of transgenic rats, which may reflect a protective response against the loss of IGF-related trophic factors. We suggest that IGF receptors may play a key role in the pathogenesis, and may have therapeutic implications in ALS. ——— amyotrophic lateral sclerosis; insulin-like growth factor; transgenic rat; IGF receptor; SOD1

Tohoku J. Exp. Med., 2008, **214** (4), 303-310.

Amyotrophic lateral sclerosis (ALS) is a fatal neurodegenerative disease caused by selective motor neuron death. Approximately 10% of cases of ALS are inherited, usually as an autosomal dominant trait. In ~25% of familial cases, the disease is caused by mutations in the gene encoding cytosolic copper-zinc superoxide dismutase (SOD1)(Aoki et al. 1993; Rosen 1993). The overexpression of mutant human SOD1 in mice is used as model for ALS, however, some experimental manipulations are difficult in transgenic (Tg) mice because of size limitations. Thus, we developed a rat model of ALS expressing a human SOD1 transgene with two ALS-associated mutations: glycine to alanine at

Received September 4, 2007; revision accepted for publication February 7, 2008.

Correspondence: Masashi Aoki, M.D., Ph.D., Department of Neurology, Tohoku University Graduate School of Medicine, 1-1 Seiryo-machi, Aoba-ku, Sendai 980-8574, Japan.
e-mail: aokim@mail.tains.tohoku.ac.jp

position 93 (G93A) and histidine to arginine at position 46 (H46R) (Nagai et al. 2001). Similar to its murine counterpart, the transgenic rats that express human SOD1 transgene ALS-associated mutations develop striking motor neuron degeneration and paralysis.

Although the mechanism of ALS is still unclear, there are many hypotheses concerning its cause of ALS, including loss of neurotrophic support to motor neurons (Rowland and Shneider 2001). The insulin-like growth factors (IGF-I and IGF-II) are neurotrophic factors expressed in the central nervous system that promote the survival and differentiation of neuronal cells including motor neurons. They could be of therapeutic value in human neurodegenerative disorders, including ALS (Adem et al. 1994; Hawkes and Kar 2003; Narai et al. 2005). Evidence that IGF-I rescues motor neurons in vitro and in animals. (Kaspar et al. 2003) has led to therapeutic trials of human recombinant IGF-I in patients with ALS (Nagano et al. 2005).

The biological actions of the IGFs are mediated through specific cell membrane receptors designated as the IGF-I and IGF-II receptors (Sepp-Lorenzino 1998; Hawkes and Kar 2003; Kim et al. 2004). Alterations of the IGF-I and IGF-II binding sites in the spinal cord of the patients with ALS would support their involvement in the pathology of ALS (Dore et al. 1996; Chung et al. 2003; Kar et al. 2006).

In the present study, we used the SOD1 (H46R) mutant Tg rat as an *in vivo* model of ALS and performed immunohistochemical studies to investigate the changes of the IGF-II receptor in the spinal cord.

Materials and Methods

Animals and clinical assessment

In this study we used nine Tg male Spargue Dawley rats as well as nine non-Tg rats (Japan SLC, Inc., Hamamatsu). The Tg rats expressing H46R mutant human copper-zinc superoxide dismutase (SOD1) were genotyped by polymerase chain reaction (PCR) assay using DNA obtained from the tail as described previously (Nagai et al. 2001). H46R Tg rats were divided into 3 groups: pre-symptomatic (aged 23 weeks, $n = 3$), onset (aged 26 weeks, just after onset, $n = 3$) and end-stage (aged 29 weeks, $n = 3$); and compared with age-matched non-transgenic littermate controls. In each Tg rat, we carefully observed the development of the symptoms of ALS. When the rats developed distinct muscle weakness in their unilateral hindlimb, they were included in the second group (onset) of the rats. All experimental protocols and procedures were approved by the Animal Committee of the Tohoku University Graduate School of Medicine, Japan.

Histopathological analysis

Nine Tg and nine control rats were anesthetized and killed by transcardial perfusion with saline and 4% paraformaldehyde in 0.1 M phosphate buffer, pH 7.4. The lumbar (L4-5) spinal cords were rapidly removed and post-fixed in the same fixative at 4°C overnight, then embedded in paraffin according to the standard protocol. Transverse sections (5 μm thick) were cut and submitted for histopathology and immunohistochemistry. A set of the sections was stained with hematoxylin and eosin (H & E).

Immunohistochemistry

For double immunohistochemistry of the spinal cord, every fifth section per animal was mounted on silanized glass slides (Dako Cytomation Co. Ltd., Gopenhagen, Denmark) and deparaffinized. The sections were quenched with 0.3% hydrogen peroxide in 10% methanol for 20 min at room temperature (RT), and rinsed in phosphate buffer saline (PBS, pH 7.4). After blocking with 5% normal serum was performed for 20 min at RT to avoid the non-specific binding of antibodies, we used the following primary antibodies: mouse anti-IGF-II receptor monoclonal antibody (1:50, overnight, 4°C; BD Transduction Laboratories, CA, USA), rabbit anti-glial fibrillary acidic protein (GFAP) polyclonal antibody (1:10,000, overnight, 4°C; Dako Cytomation Co. Ltd.), and rabbit anti-ionized calcium-binding adapter molecule-1 (Iba-1) polyclonal antibody (1:3,000, overnight, 4°C; Wako Pure Chemicals, Osaka). After incubation with a mixture of biotinylated anti-mouse and anti-rabbit IgG secondary antibodies (1:400, 1 hr, RT; Vector Laboratories, Burlingame, CA, USA), the immunoreactivity was enhanced with avidin-biotin peroxidase complex (ABC) kit (Vector Laboratories). We used two kinds of color substrates as a chromogen. For the visualization of the IGF-II receptor we used 3,3-diaminobenzidine and nickel (blue-gray color), which was the first staining of the double immunostain-

ing (Vector Laboratories). For the staining of GFAP and Iba1 we used Nova Red (light-red color), which was the second staining of the double immunostaining (Vector Laboratories). To prevent cross-reaction between the first and the second immunoreactivities, we performed the double immunohistochemistry sequentially, and used an avidin-biotin blocking kit (Vector Laboratories) between the two sets of immunohistochemistry.

Quantitative analysis

Sections were examined and microphotographed under a light microscope (at 200 × magnification, Olympus BX50). We evaluated a total of five transverse sections from three different rats at each stage. The estimated motor neuron counts were performed on HE-stained sections in the lumbar spinal cord. Cells were selected as motor neurons if they were > 30 μm in diameter, multipolar with neuronal morphology, and located in the anterior horn of the spinal cord. The resulting data provided the estimated number of motor neurons per unilateral anterior horn. For semi-quantification of the double immunohistochemistry, we counted the double-immunoreactive areas in the photographed digital images of the anterior horns (60 × 45 μm for 2,048 × 1,536 pixels) using Image J software (National Institutes of Health, Bethesda, MD, USA). The average area (pixels/μm) double immunoreactive for IGF-II receptor and GFAP in the unilateral anterior horn in each rat was used for statistical analysis.

Statistical analysis

Values are expressed as the means ± S.D. The statistical analysis was performed using GraphPad PRISM (San Diego, CA, USA). Differences among the experimental groups were examined for significance using one way analysis of variance (ANOVA) among means of value with the group of rats as the independent factor. We tested multiple pair-wise comparisons between means by Bonferroni-Dunn post hoc test.

Results

The clinical course of transgenic rats

The Tg rats expressing the human SOD1 mutant (H46R) developed motor neuron disease with the onset of this clinical weakness at a mean age of around 180 days. Clinically apparent weakness, denoted by dragging of one hindlimb without limb tremor, was evident somewhat later. Simultaneously with the onset of clinical weakness, the affected rats showed prominent weight loss. While the initial clinical manifestation of weakness was unilateral leg paralysis, this progressed and became bilateral in the H46R Tg rats. In the early stages of the illness, another distinctive abnormality was increased tone in the tail musculature, resulting in an elevated, segmentally spastic tail posture. As the disease progressed, the rats exhibited marked muscle wasting in the hind limbs, typically dragging themselves about the cage using the forelimbs. Thereafter, the forelimbs also became weak, in association with further weight loss. At the end-stage, the affected rats could not drink water and died. The mean age of death was around 200 days.

We estimated the numbers of motor neurons in each anterior horn of the control littermates and

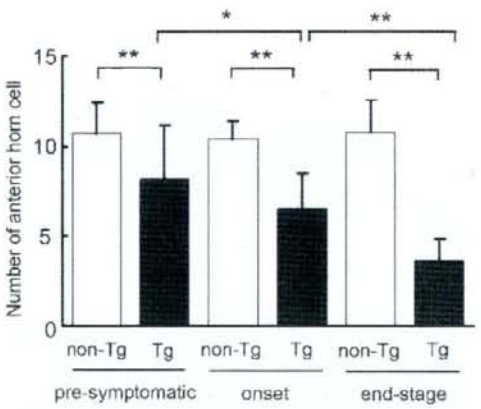

Fig. 1. Numbers of anterior horn cells: Numbers of anterior horn cells in the lumbar spinal cord at the pre-symptomatic, onset and end-stage. Mean number of the anterior horn cells from non-Tg rats (*open bar*) and H46R Tg rats (*solid bar*) are presented. The estimated numbers of motor neurons in the anterior horn of the spinal cord were almost the same in the control rats, while those in the Tg rats were gradually decreased: pre-symptomatic stage non-Tg, 10.7 ± 1.7; Tg, 8.3 ± 3.0 anterior horn cells/slice; onset stage non-Tg, 10.4 ± 1.0; Tg, 6.5 ± 1.9 anterior horn cells/slice; end-stage non-Tg, 10.8 ± 1.8; Tg, 3.6 ± 1.3 anterior horn cells/slice. Bonferroni-test $^{**}p < 0.01$; $^{*}p < 0.05$. The error bars denote the S.D.

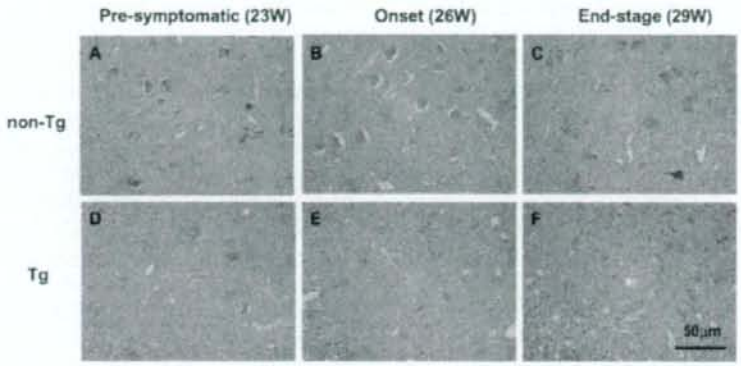

Fig. 2. Anterior horn cells with hematoxylin and eosin staining: Decreased number of anterior horn cells in the anterior horn of the lumbar spinal cord in non-Tg rats and H46R Tg rats at pre-symptomatic, onset and end-stage. Sections were stained with hematoxylin and eosin. Scale bar: 50 μm. Note that a decrease in the number of anterior horn cells in the lumbar spinal cord is evident at the pre-symptomatic stage in H46R Tg rats.

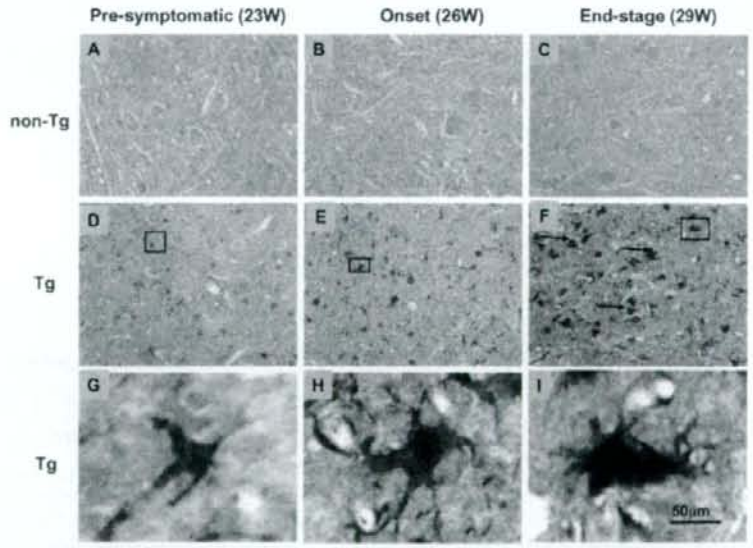

Fig. 3. Double-immunostaining for IGF-II receptor and GFAP: Double-immunostaining for Insulin-like growth factor-II (IGF-II) receptor and glial fibrillary acidic protein (GFAP) in non-Tg rats and H46R Tg rats at pre-symptomatic, onset and end-stage. Scale bar: 50 μm. IGF-II receptor and GFAP double-positive cells were found in the anterior horns of the lumbar spinal cord, and were co-stained with GFAP in the end-stage (F, I) of H46R Tg rats (arrows). The co-localization of IGF-II receptor and GFAP were visualized as a dark-red using Nova Red and DAB+Nickel chromogen (I). While there was evidence of GFAP-immunoreactive astrocytes in the pre-symptomatic stage (D, G) and at the onset (E, H), these reactive astrocytes were colored only light-red (G, H), indicating that the cells visualized were GFAP positive only.

Tg rats as a function of age. As indicated in Fig. 1, the estimated numbers declined abruptly in parallel with the development of clinical paralysis. In the spinal cords of the Tg rats, the drop-off in estimated motor neuron numbers preceded the onset of clinical weakness.

Histopathological studies in the spinal cords

The H46R Tg rats exhibited neuropathological abnormalities associated with the degeneration of motor neurons in the anterior horns of the spinal cord (Fig. 2). They also showed evidence of proliferation of small non-neuronal cells with the morphological characteristics of astroglia and microglia. In the pre-symptomatic stage at 23 weeks of age, the numbers of large, multipolar neurons in the anterior horn (motor neurons) were decreased (Fig. 2D) as compared to non-Tg littermates (Fig. 2A) , while the numbers of hypertrophic astrocytes were increased (Fig. 2D). By 26 weeks of age, when clinical weakness became apparent, there was a marked loss of large, multipolar neurons (Fig. 2E) as compared to non-Tg littermates (Fig. 2B). At that time, numerous hypertrophic astrocytes and microglia were evident in all stages of transgenic rats, as were sites of swelling in axons in the anterior horn (Fig. 2E). Many inclusions were characterized by a dense core and clear peripheral halo, strongly resembling the Lewy body-like hyaline inclusions seen in the spinal cords of human ALS patients. These were detected in the neuropil, motor neurons, and astrocytes (data not shown). At 29 weeks of age, corresponding to the end-stage when the H46R Tg rats clinically displayed quadriplegia or a moribund state, the rats of this end-stage showed severe loss of the anterior horn cells with gliosis of the spinal cords (Fig. 2E).

Immunohistochemical analyses for IGF-II receptor

In the anterior horn of the spinal cord of the H46R Tg rats, immunohistochemistry using the antibody against the IGF-II receptor showed intensely stained IGF-II receptor-positive glial cells with the appearance of astrocytes, but few IGF-II receptor-positive glial cells were observed in the spinal cord of the non-Tg littermates (Fig. 3), which were evident at the end-stage in H46R Tg rats (Fig. 3F). However, there were not evident at the pre-symptomatic stage (Fig. 3D) or at the onset of the disease (Fig. 3E). The IGF-II receptor-positive cells showing the morphology of astrocytes were confirmed as astrocytes by double-stained immunohistochemistry using the antibody against GFAP, which is a specific marker for astrocytes. There was a 125-fold increase in IGF-II receptor/GFAP double positive areas in the anterior horn of the spinal cord of the H46R Tg rats as compared to non-Tg littermates using ImageJ software on images captured electronically (Fig. 4). This increase was statistically significant ($p < 0.001$). IGF-II receptor-positive cells were not stained simultaneously with Iba1, which is a specific marker for microglia, in both Tg (Fig. 5D-I) and non-Tg (Fig. 5A-C) rats. In the spinal cord of non-Tg rats, few IGF-II receptor-positive astrocytes were detected although some IGF-II receptor-positive neurons were observed in the anterior horn.

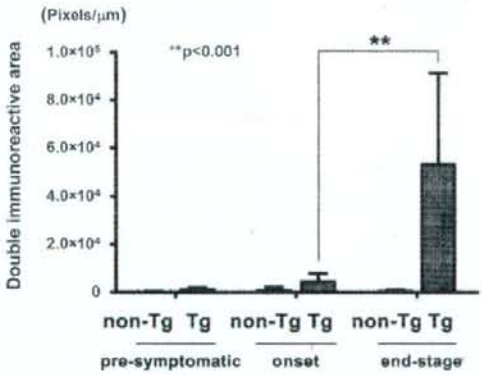

Fig. 4. Volume of double-positive areas of IGF-II receptor and GFAP: Volume of double-positive areas (pixels/μm) of insulin-like growth factor-II (IGF-II) receptor and glial fibrillary acidic protein (GFAP) in the anterior horn of the lumbar spinal cord. IGF-II receptor and GFAP double-positive area was significantly ($^{**}p < 0.001$) increased in the anterior horn of the lumbar spinal cord in the end-stage of ALS transgenic rats.

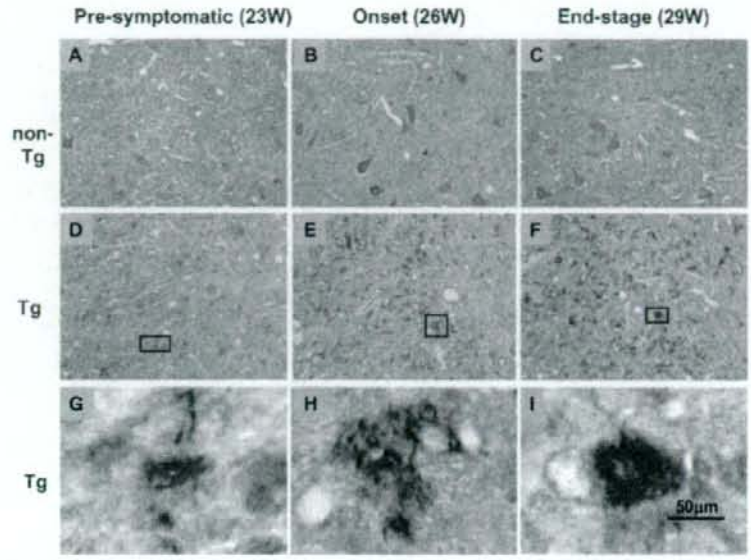

Fig. 5. Double-immunostaining for IGF-II receptor and Iba1: Double-immunostaining for insulin-like growth factor-II (IGF-II) receptor and ionized calcium-binding adapter molecule-1 (Iba1) in the anterior horn of the lumbar spinal cord from non-Tg rats and H46R Tg rats at pre-symptomatic, onset and end-stage. Scale bar: 50 μm. Iba1-immunoreactive microglia were visualized as light-red due to Nova RED chromogen in Tg rats at pre-symptomatic (D, G), symptomatic (E, H) and end-stage (F, I). However, there were no IGF-II receptor and Iba1 double positive cells, which would be colored by both Nova Red and DAB + Nickel color substrates.

Discussion

Our results showed the apparent loss of motor neurons in the anterior horn of the lumbar spinal cord in H46R Tg rats as described in our previous report (Nagai et al. 2001). We estimated the numbers of motor neurons in each anterior horn of the Tg rats as well as in control littermates and confirmed that the estimated number declined abruptly in parallel with the development of clinical paralysis. The H46R Tg rats also showed evidence of proliferation of small non-neuronal cells with the morphological characteristics of astroglia and microglia.

Various growth factors and their receptors are expressed differentially in ALS. The insulin-like growth factors are neurotrophic factors expressed in the central nervous system that promote the survival and differentiation of neuronal cells including motor neurons. The ability of IGFs to enhance the outgrowth of spinal motor neurons makes it a potential therapeutic agent for patients with ALS (Kaspar et al. 2003). Several studies have reported positive effects of IGF-I in reducing motor neuron death, delaying the onset of motor performance decline and the increasing life span in SOD1 mouse models of ALS and in one clinical trial. The IGF-1 studies in humans have reported that the progression of functional impairment in patients receiving high doses of IGF-1 was reduced by 26% vs patients receiving placebo (Lai et al. 1997). However, a second clinical trial produced no positive results (Borasio et al. 1998), and there currently is a phase III randomized, double-blind, placebo-controlled clinical IGF-1 trial underway. Therefore, we examined further the expression of the receptors of IGFs in the model of ALS.

A number of studies suggested that the level of expression of IGF receptors in reactive astro-

cytes was increased with the disease progression in human ALS, SOD1 Tg rats and mice (Adem et al. 1994; Chung et al. 2003). During development, astrocytes have been recognized as a source of cytokines that are involved in the growth and differentiation of neuronal cells and glial cell populations (Raff et al. 1985; Du and Dreyfus 2002). Recently, using immunohistochemistry, apparent increases of IGF-I receptors in reactive astrocytes in the anterior horns of the spinal cord in SOD1 G93A Tg mice were observed (Chung et al. 2003). The IGF-II receptor is a multifunctional single transmembrane glycoprotein that, along with the cation-dependent M6P (CD-M6P) receptor, mediates the trafficking of M6P-containing lysosomal enzymes from the trans-Golgi network to lysosomes. In the present study, immunohistochemistry using the antibody against the IGF-II receptor showed intensely stained IGF-II receptor-positive glial cells with the appearance of astrocytes in the anterior horn of the spinal cord of the H46R Tg rats. This was evident at the end-stage, however, but not evident at the pre-symptomatic stage or at the onset of the disease. The IGF-II receptor- positive glial cells showing the morphology of astrocytes were confirmed to be astrocytes by double-stained immunohistochemistry using the antibody against GFAP. This result was compatible with the expression of IGF-I receptors in Tg mice (Chung et al. 2003). On the other hand, we observed Iba1 reactive hypertrophic microglia in the pre-symptomatic, onset and end-stage of the Tg rats. However, IGF-II receptor-positive reactive microglia were not observed in the H46R Tg rats, although Kihira T and co-workers (Kihira et al. 2007) reported that some microglia expressing IGF-II have neuroprotective effects on the motor neurons in patients with ALS.

The apparent increase in IGFI and II receptors in the anterior horn in ALS spinal cords may be due to the loss of IGF-related trophic factors leading to receptor upregulation in an attempt to maintain neuronal homeostasis and insure neuronal survival. This study suggests that the expression of IGF receptors may play a key role in the pathogenesis, and that IGFs may have therapeutic applications in ALS.

Acknowledgments

This work was supported by Grant-in-Aid for Scientific Research (C: 19590977) from the Ministry of Education, Culture, Sports, Science, and Technology, Japan and a grant from the Ministry of Health, Labor, and Welfare, Japan (M.A., Y.I.). Research funding was also provided by the Haruki ALS Research Foundation (M.A., H.W., Y.I.).

References

Adem, A., Ekblom, J., Gillberg, P.G., Jossan, S.S., Hoog, A., Winblad, B., Aquilonius, S.M., Wang, L.H. & Sara, V. (1994) Insulin-like growth factor-1 receptors in human spinal cord: changes in amyotrophic lateral sclerosis. *J. Neural. Transm. Gen. Sect.*, **97**, 73-84.

Aoki, M., Ogasawara, M., Matsubara, Y., Narisawa, K., Nakamura, S., Itoyama, Y. & Abe, K. (1993) Mild ALS in Japan associated with novel SOD mutation. *Nat. Genet.*, **5**, 323-324.

Borasio, G.D., Robberecht, W., Leigh, P.N., Emile, J., Guiloff, R.J., Jerusalem, F., Silani, V., Vos, P.E., Wokke, J.H. & Dobbins, T. (1998) A placebo-controlled trial of insulin-like growth factor-I in amyotrophic lateral sclerosis. European ALS/IGF-I Study Group. *Neurology*, **51**, 583-586.

Chung, Y.H., Joo, K.M., Shin, C.M., Lee, Y.J., Shin, D.H., Lee, K.H. & Cha, C.I. (2003) Immunohistochemical study on the distribution of insulin-like growth factor I (IGF-I) receptor in the central nervous system of SOD1(G93A) mutant transgenic mice. *Brain Res.*, **994**, 253-259.

Dore, S., Krieger, C., Kar, S. & Quirion, R. (1996) Distribution and levels of insulin-like growth factor (IGF-I and IGF-II) and insulin receptor binding sites in the spinal cords of amyotrophic lateral sclerosis (ALS) patients. *Brain Res. Mol. Brain Res.*, **41**, 128-133.

Du, Y. & Dreyfus, C.F. (2002) Oligodendrocytes as providers of growth factors. *J. Neurosci. Res.*, **68**, 647-654.

Hawkes, C. & Kar, S. (2003) Insulin-like growth factor-II/mannose-6-phosphate receptor: widespread distribution in neurons of the central nervous system including those expressing cholinergic phenotype. *J. Comp. Neurol.*, **458**, 113-127.

Kar, S., Poirier, J., Guevara, J., Dea, D., Hawkes, C., Robitaille, Y. & Quirion, R. (2006) Cellular distribution of insulin-like growth factor-II/mannose-6-phosphate receptor in normal human brain and its alteration in Alzheimer's disease pathology. *Neurobiol. Aging*, **27**, 199-210.

Kaspar, B.K., Llado, J., Sherkat, N., Rothstein, J.D. & Gage, F.H. (2003) Retrograde viral delivery of IGF-1 prolongs survival in a mouse ALS model. *Science*, **301**, 839-842.

Kihira, T., Suzuki, A., Kubo, T., Miwa, H. & Kondo, T. (2007) Expression of insulin-like growth factor-II and leukemia inhibitory factor antibody immunostaining on the ionized calcium-binding adaptor molecule 1-positive microglias in the spinal cord of amyotrophic lateral sclerosis patients. *Neuropathology*, **27**, 257-268.

Kim, B., van Golen, C.M. & Feldman, E.L. (2004) Insulin-like growth factor-I signaling in human neuroblastoma cells. *Oncogene*, **23**, 130-141.

Lai, E.C., Felice, K.J., Festoff, B.W., Gawel, M.J., Gelinas, D.F., Kratz, R., Murphy, M.F., Natter, H.M., Norris, F.H. & Rudnicki, S.A. (1997) Effect of recombinant human insulin-like growth factor-I on progression of ALS. A placebo-

controlled study. The North America ALS/IGF-I Study Group. *Neurology*, **49**. 1621-1630.

Nagai, M., Aoki, M., Miyoshi, I., Kato, M., Pasinelli, P., Kasai, N., Brown, R.H., Jr. & Itoyama, Y. (2001) Rats expressing human cytosolic copper-zinc superoxide dismutase transgenes with amyotrophic lateral sclerosis: associated mutations develop motor neuron disease. *J. Neurosci.*, **21**. 9246-9254.

Nagano, I., Ilieva, H., Shiote, M., Murakami, T., Yokoyama, M., Shoji, M. & Abe, K. (2005) Therapeutic benefit of intrathecal injection of insulin-like growth factor-1 in a mouse model of Amyotrophic Lateral Sclerosis. *J. Neurol. Sci.*, **235**. 61-68.

Narai, H., Nagano, I., Ilieva, H., Shiote, M., Nagata, T., Hayashi, T., Shoji, M. & Abe, K. (2005) Prevention of spinal motor neuron death by insulin-like growth factor-1 associating with the signal transduction systems in SODG93A transgenic mice. *J. Neurosci. Res.*, **82**. 452-457.

Raff, M.C., Abney, E.R. & Fok-Seang, J. (1985) Reconstitution of a developmental clock in vitro: a critical role for astrocytes in the timing of oligodentrocyte differentiation. *Cell*, **42**. 61-69.

Rosen, D.R. (1993) Mutations in Cu/Zn superoxide dismutase gene are associated with familial amyotrophic lateral sclerosis. *Nature*, **364**. 362.

Rowland, L.P. & Shneider, N.A. (2001) Amyotrophic lateral sclerosis. *N. Engl. J. Med.*, **344**. 1688-1700.

Sepp-Lorenzino, L. (1998) Structure and function of the insulin-like growth factor I receptor. *Breast Cancer Res. Treat.*, **47**. 235-253.

***** 事務局 *****
東北大学大学院医学系研究科神経内科
〒980-8574 仙台市青葉区星陵町 1-1
電話 022-717-7189 / Fax 022-717-7192